

Enhancement of Bone Regeneration and Graft Material Resorption Using Surface-Modified Bioactive Glass in Cortical and Human Maxillary Cystic Bone Defects

Ahmed El-Ghannam, PhD¹/Hany Amin, DMD, MD²/Tamer Nasr, DMD³/Ashraf Shama, MD⁴

Purpose: Bioactive glass bonds to bone through a calcium phosphate layer that mimics the structure of the mineral phase of bone. Formation of this layer is inhibited in the presence of serum protein. The authors hypothesize that creation of a calcium phosphate layer on the surface of bioactive glass before implantation will enhance bone regeneration and graft material resorption in bone defects.

Materials and Methods: Bioactive glass particles covered with a layer of amorphous calcium phosphate (BG-ACP), bioactive glass particles covered with a layer of hydroxycarbonate apatite (BG-HCA), and unmodified bioactive glass particles (as a control) were prepared and implanted in cortical bone defects in dogs or in human maxillary cavities. Ungrafted sites were also used as a control. **Results:** Histomorphometric analyses showed significantly more bone tissue regeneration and graft material resorption in the defects filled with BG-HCA than in those filled with BG-ACP or unmodified bioactive glass ($P < .0001$). Moreover, measurements of radiographic density of the grafted areas suggested a higher rate of bone regeneration in defects filled with the modified bioactive glass than in those filled with unmodified bioactive glass or in the ungrafted control. Bone formation was significantly greater in defects filled with unmodified bioactive glass particles than in ungrafted defects. **Discussion:** The enhancement of bone regeneration could be explained by the ability of the apatite layer to facilitate bone adsorption and enhance calcium release, which stimulates osteoblast differentiation and bone formation. **Conclusion:** Results of both the clinical and animal studies suggest that the use of surface-modified bioactive glass covered with a hydroxycarbonate apatite layer has the potential to accelerate bone formation and graft material resorption better than unmodified bioactive glass. *INT J ORAL MAXILLOFAC IMPLANTS* 2004;19:184–191

Key words: bioactive glass, bone graft, dental radiography, histomorphometry

Synthetic grafts such as bioactive glass and calcium phosphate (CaP) ceramics are commonly used in oral, maxillofacial, and orthopedic surgery

for various indications, such as the filling of bone cavities, augmentation for dental implants, and reconstruction of bone lost during tumor removal or trauma.^{1–3} In particular, bioactive glass forms a quick bond with bone through a hydroxyapatite layer that forms on the material surface.⁴ Fortunately, this bioactive hydroxyapatite layer can be formed on the bioactive glass surface even in acellular simulated body fluid (SBF) with ion concentrations nearly equal to those of human blood plasma. Formation of the hydroxycarbonate apatite (HCA) layer has been reported to be fastest for implants with the highest level of bioactivity.^{4,5}

Currently, the mechanism governing bioactive behavior in vivo is not fully understood. Research has been conducted with bioactive glass to understand the bioactivity mechanisms at work by studying its reaction to immersion in SBFs.⁵ The results of these

¹Assistant Professor, University of Kentucky, Center for Biomedical Engineering, Wenner Gren Research Laboratory, Graduate School, Center for Oral Health Research, School of Dentistry, Lexington, Kentucky.

²Professor, Cairo University, Faculty of Dental Medicine, Department of Oral Surgery, Cairo, Egypt.

³Lecturer, Cairo University, Faculty of Dental Medicine, Department of Oral Surgery, Cairo, Egypt.

⁴Assistant Professor, Cairo University, Faculty of Veterinary Medicine, Department of Surgery, Cairo, Egypt.

Correspondence to: Dr Ahmed El-Ghannam, University of Kentucky, Center for Biomedical Engineering, Wenner Gren Research Laboratory, Graduate School, Center for Oral Health Research, School of Dentistry, Lexington, KY 40506-0070. Fax: +859-257-1856. E-mail: arelgh2@uky.edu

studies suggest that after bioactive glass is exposed to body fluids, alkali ions are leached from the glass in a preferential manner, resulting in the formation of a silica-rich layer that facilitates the deposition of amorphous CaP (ACP) on the surface of bioactive glass. Subsequently, the ACP layer crystallizes into a calcium-deficient HCA similar to bone in its mineral phase.⁶ It should be noted that the behavior of bioactive glass in SBF is totally different from its behavior in tissue fluids because of differences in composition and because of fluid turnover with tissue fluids in vivo. Tissue fluid contains proteins that actively inhibit the formation of the HCA layer; SBF does not.⁷ Thus, in vivo formation of a mineralized ACP layer at the tissue-material interface may not be explained by the simple dissolution-precipitation mechanism. In fact, when bioactive glass was immersed in a protein-containing medium, surface mineralization of bioactive glass occurred only in the presence of bone cells.⁷

A recent study by El-Ghannam and coworkers indicated that the greater bioactive effect of the surface-modified bioactive glass as compared to unmodified bioactive glass (UBG) or hydroxyapatite ceramic was the result of the ability of the HCA layer to concentrate active fibronectin on its surface.⁸ Matsuoka and associates demonstrated that an HCA layer created prior to cell seeding on the surface of apatite-wollastonite (A-W) glass ceramic provided a bone-cell-like environment with the large pool of calcium ions necessary for osteogenic differentiation.⁹

The ability to create an HCA layer on the surface of biomaterials is highly significant because HCA-coated implants have demonstrated increased bone-bonding ability.¹⁰⁻¹³ The authors hypothesize that the creation of an HCA layer on the surface of bioactive glass before implantation will enhance bone regeneration and graft material resorption inside bone defects. In the present study, bone regeneration and graft material resorption in cortical bone defects filled with bioactive glass particles with a layer of ACP (BG-ACP), bioactive glass particles with a layer of HCA (BG-HCA), or UBG particles or left ungrafted were compared. In addition, the effect of grafting with surface-modified bioactive glass on bone tissue regeneration in human cystic bone defects was evaluated using a direct radiographic image technique.

MATERIALS AND METHODS

Bioactive Glass Preparation

Bioactive glass (4555, Bony Glass; BECO, Cairo, Egypt) was prepared by mixing appropriate amounts

of silica (SiO₂), calcium carbonate (CaCO₃), sodium carbonate (Na₂CO₃), and calcium phosphate (CaHPO₄). The mixed glass was melted in a platinum crucible at 1350°C. The homogeneity of the glass was assured by swirling the melt 8 times over a 4-hour period. The glass was quenched in deionized water, dried, ground, and sifted. Bioactive glass particles between 150 and 350 μm in diameter were selected for the study.

Surface Modification and Characterization

The surface chemistry of the bioactive glass was modified by immersion in SBF which is similar in composition and ion concentration to plasma. One batch of bioactive glass particles was immersed in SBF at 37°C for 24 hours, another was immersed for 96 hours. After immersion, the surface of bioactive glass was analyzed by Fourier transform infrared spectroscopy (FTIR). FTIR analyses confirmed the formation of an ACP layer after 24 hours and an HCA layer after 96 hours.

Animal Study

Surgery Procedures. Nine 3- to 4-month-old mongrel dogs weighing 5 to 6 kg each were selected for the study. In each dog, 2 cylindrical cores of corticocancellous bone were surgically removed from one of the tibias. Intramuscular injections of anesthesia were given prior to the surgical procedure. Incisions were made over the shaft of the proximal upper third of the tibia to expose its proximal medial aspect. The exposed bone was drilled in the coronal plane from the medial to the lateral cortical surface using a low-speed, saline-cooled drill in a stepwise fashion (ie, drill bits were incrementally increased from 1.0 to 10 mm in diameter in 1.0-mm increments). A second 10-mm-wide hole was drilled 2 cm away from the first hole. The bone marrow chamber was evacuated by repeated washings with saline through a syringe introduced into the defect space. The surgical site was packed with gauze until bleeding subsided. Following ablation, 1 hole in each dog was filled with BG-ACP, BG-HCA, or UBG particles. The other hole was left empty for comparison. At 6 weeks postsurgery the animals were sacrificed and the bone segments containing the defects were bisected and processed for histologic analysis.

Histologic Analysis. Immediately following sacrifice, the lateral distal tibias were fixed in 10% neutral buffered formalin for 24 hours, then in Zenker's fluid for 24 hours, and then in Bouin's fluid for 24 hours. The samples were decalcified in trichloroacetic acid and dehydrated in ascending grades of ethyl alcohol. Then the samples were cleared in

benzene, embedded in paraffin wax, sectioned into thin slices (5 to 7 μm long), and stained with Harris' hematoxylin and eosin. Bone tissue formation inside the defects was analyzed using a microscope.

Histomorphometry. Photos of the sections were taken, and these photos were analyzed. To determine the effect of surface modification of bioactive glass on bone regeneration and graft material resorption, the areas of tissue, of cells, and of graft material inside the defect were calculated. The areas of the 3 regions were quantified utilizing Photoshop 6.0 (Adobe, San Jose, CA) and image-processing software (Image Processing Tool Kit; Reindeer Games, Asheville, NC). The images first had to be divided into regions to obtain binary images. Regional segmentation was accomplished using intensity thresholding, with images in the hue, saturation, and intensity (HSI) format. In some cases, the Haralick 1 texture operator¹⁴ and intensity thresholding were used in combination. The Haralick texture operator calculates the difference moment in the image, thus using texture to separate the bony and cellular regions.¹⁴ Other techniques attempted for segmentation could not properly separate the cellular and bony regions because the grayscale and color intensities were very similar between bony and cellular regions. Morphologic open and close techniques were applied to the binary bioactive glass images to eliminate most of the small artifacts and false holes in the images. Then each area was measured. The Global Measurement Filter (Image Processing Tool Kit; Reindeer Games) was used to calculate the percentages of black pixels representing materials, cells, and tissue.

Clinical Study

Patient Selection. Thirty patients diagnosed with an intrabony radicular cyst in the anterior maxilla were selected from the outpatient clinic of the Oral Surgery Department, Cairo University. The cysts were 2 to 4 inches in diameter. The patients had not complained of any systemic disease and were not receiving any medical treatment. They were divided into 3 groups of 10 patients, with 6 men and 4 women in each group. The cavity that remained after cyst enucleation was filled with either BG-HCA (in group 1) or UBG (in group 2). In group 3, the cavity that remained after cyst enucleation was not grafted.

Operative Procedures. An infraorbital nerve block and an incisive canal nerve block were induced by anesthesia. After securing anesthesia, a mucoperiosteal flap was created and reflected under completely aseptic conditions. The underlying bone was removed and the apical lesion was curetted. The surgical site was irrigated with sterile saline and

bleeding, if present, was arrested by application of a gauze pack. In groups 1 and 2, the graft material was loosely packed inside the bony defect so that it was flush with the bony margins, with no overcontouring. Care was taken to ensure that no bioactive glass particles were placed outside the cavity under the mucoperiosteal flap. In group 3, the cavities were not grafted. The flap was repositioned and sutured. Gentle pressure with a sterile gauze pack was applied postoperatively to the surgical flap to facilitate reattachment of the flap to the underlying bone. In all cases, postoperative antibiotics and an anti-inflammatory agent were prescribed.

Clinical Evaluation. Follow-up examinations were conducted 1 day postsurgery, 7 days postsurgery (at the time of suture removal), and 2, 4, 8, 16, and 24 weeks postsurgery. Mucosal color and any postoperative pain or swelling were noted during clinical evaluations.

Intraoral Digital Radiographic Imaging. At 2, 4, 8, and 16 weeks postsurgery the mean density of the image of the surgical defect was measured using a Digora unit (Soredex, Helsinki, Finland). The mean density values and standard deviations were calculated using QuatroPro software (Corel, Ottawa, Ontario, Canada).

Statistical Analysis. Statistical comparison was made using Microstat (JCE Software, Madison, WI) and QuatroPro software. The mean values and standard deviations of each parameter were calculated. The differences between means were evaluated using the Student *t* test; $P < .05$ was considered significant.

RESULTS

Animal Study

Histology. UBG. Figure 1a shows a stained histologic section from the tibia of a dog that was grafted with UBG. There are 3 distinct areas in the section—UBG, calcified spongy bone tissue, and areas of cellular expansion prior to bone formation. New bone tissue formed directly on the surface as well as in cavities and cracks in the particles. In contrast, the ungrafted cavities, the other controls, were filled with marrow spaces and showed minimal bone tissue formation. After regional segmentation of the image shown in Fig 1a using the Haralick 1 texture operator, the spongy bone appeared purple, areas of cellular expansion appeared brown, and UBG appeared white (Fig 1b). Figures 1c to 1e show the individual binary images created by intensity thresholding of the UBG particles, the spongy bone, and the cellular regions, respectively.

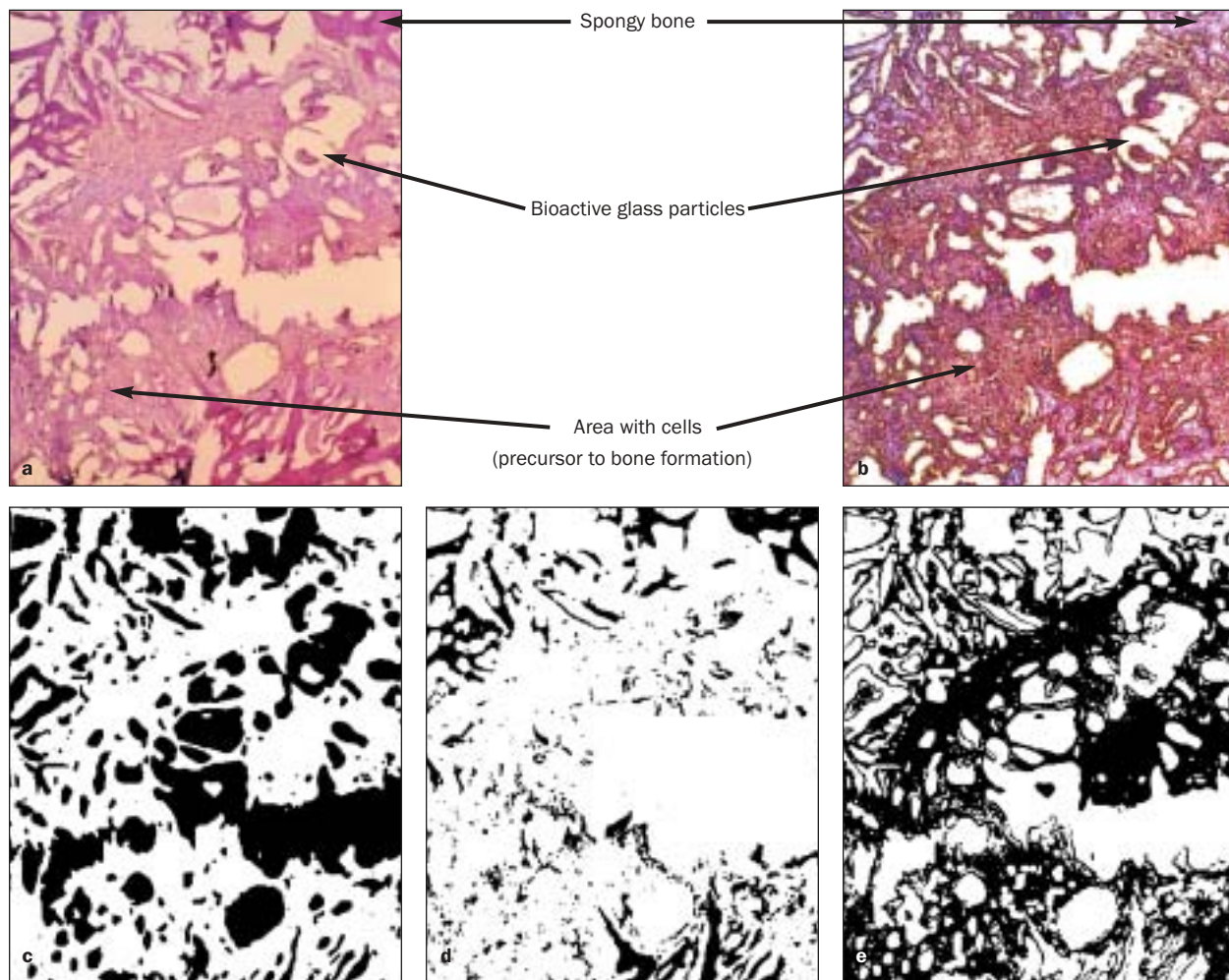


Fig 1 (a) Stained histologic section from the tibia of a dog that was grafted with UBG particles for 6 weeks. A large amount of cellular activity around the glass particles can be seen in the middle of the defect. (b) The image after regional segmentation using the Haralick 1 texture operator. (c to e) The individual binary images, created by intensity thresholding, for the bioactive glass particles, spongy bone, and cellular regions, respectively.

BG-ACP. Figure 2a shows a histologic section of a bone defect in the tibia of a dog grafted with BG-ACP 6 weeks postsurgery. BG-ACP particles were cemented with the newly formed bone tissue (Fig 2a). Many particles in the middle of the cavity were filled with bone tissue and cells. A large amount of cellular activity was seen in the middle of the cavity, especially around the graft material. Most of the particles inside the defect were excavated and filled with bone tissue, osteocytes, or both. Converting the image in Fig 2a to the HSI format before thresholding resulted in binary images of the BG-ACP particle, bone tissue, and cellular regions (Figs 2b to 2d). These images were used to calculate the percentage of bone and graft material in every defect.

BG-HCA. Figure 3a shows a histologic section of a bone defect in the tibia of a dog grafted with BG-HCA 6 weeks postsurgery. The defect was filled

with new bone with a trabecular architecture and had incorporated bioactive glass particles into its structure. A minimal amount of graft material was observed. In the segmented image in Fig 3b, the cellular regions are clearly distinguished by their red color. The bony region is characterized by both pink and white regions because of the channels found in trabecular bone. BG-HCA particles also appear white in this image; their area was subtracted during the surface area calculations.

Histomorphometry. Histomorphometric analysis showed that the percentage of bone was significantly higher in the defects filled with BG-HCA than in defects grafted with BG-ACP ($P < .0001$). Defects filled with BG-ACP demonstrated significantly greater bone tissue formation than those filled with UBG ($P < 0.01$) (Fig 4). The calculation of the percent area occupied by graft material inside the

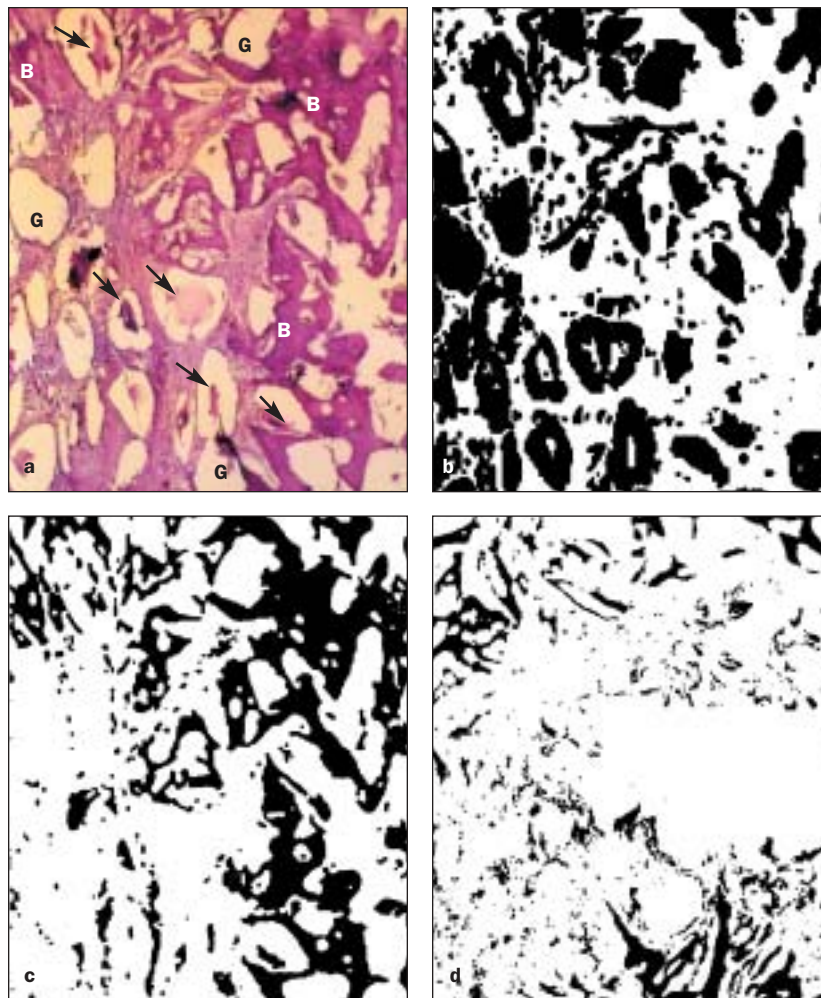


Fig 2 (a) Histologic section of a bone defect in the tibia of a dog grafted with BG-ACP 6 weeks postsurgery. New bone (B) was formed on the surface of the BG-ACP particles (G). Many particles were excavated and filled with bone tissue (arrows). Binary images of (b) the BG-ACP particles, (c) bone tissue, and (d) cellular regions were created by converting the images shown in (a) to the HSI format.

defect showed that the area occupied by UBG was significantly higher than that occupied by BG-ACP ($P < .001$; Fig 4). In addition, the area occupied by BG-ACP was significantly greater than that occupied by BG-HCA ($P < .001$).

Clinical Study

Clinical Observation. Clinical examination 1 day postsurgery showed that patients in groups 1 and 2 demonstrated more edema than patients in group 3. The overlying mucosa had the same reddish color in all patients. At the time of suture removal, the mucosa of all patients had regained normal color and contour. Moreover, no flap dehiscence was observed.

Digital Radiographic Imaging. Figure 5 shows the mean radiographic density of the images of the grafted and ungrafted cystic bone defects after 2, 4, 8, 16, and 24 weeks of implantation. The rate of increase in density in the defects grafted with BG-

HCA was more than double that in defects grafted with UBG throughout the first 2 to 4 weeks postsurgery. In contrast, there was a significant decrease in density in the ungrafted control defects during the same time period. The density of defects filled with BG-HCA continued to increase until it reached its maximum at week 16 (Fig 5) and then decreased. The density inside the defects filled with BG-HCA decreased significantly between weeks 16 and 24 ($P < .01$). On the other hand, the density of defects filled with UBG and the control defects continued to increase.

DISCUSSION

This study showed that the biologic performance of bioactive glass can be improved by surface modification. The creation of an HCA layer on the surface of bioactive glass before implantation promoted

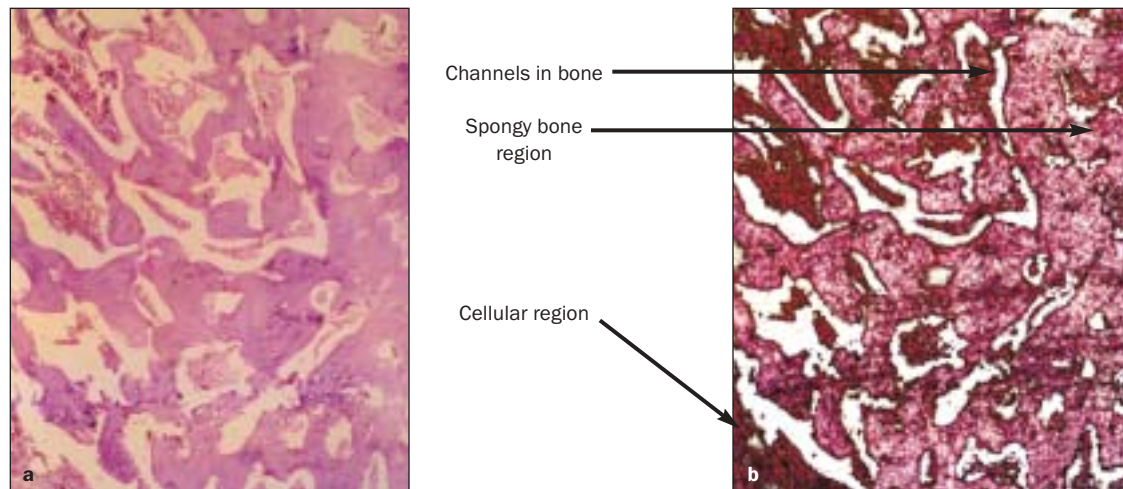


Fig 3 (a) Histologic section of a bone defect in the tibia of a dog grafted with BG-HCA 6 weeks postsurgery. (b) The image after regional segmentation. The cellular regions are clearly distinguished by their red color. The bony region is characterized by both the pink and white regions. BG-HCA also appears white in this image.

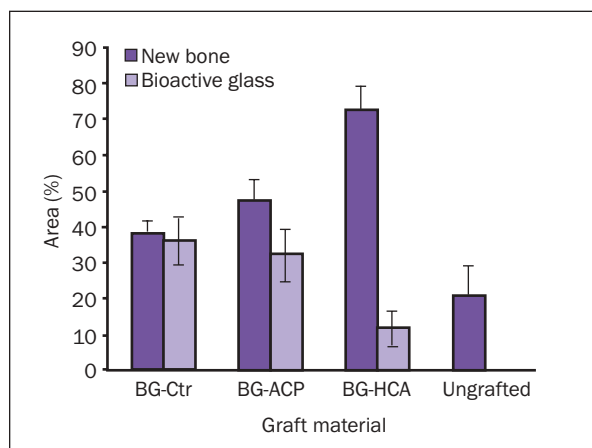


Fig 4 Histomorphometric analysis of the percent bone and graft material within the defects created in the tibias of the dogs 6 weeks postsurgery. The percentage of bone within the defects filled with BG-HCA was significantly higher than that present in defects filled with BG-ACP ($P < .0001$).

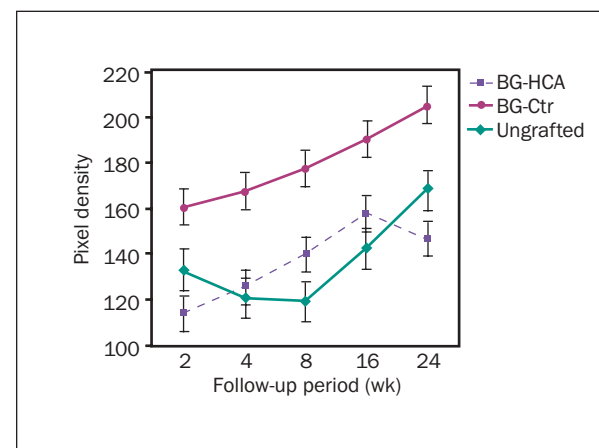


Fig 5 The mean radiographic density of the images of the grafted and ungrafted cystic bone defects after 2, 4, 8, 16, and 24 weeks of implantation. The increase in density was the result of new bone tissue formation.

bone tissue regeneration and graft material resorption in cortical bone defects and maxillary cystic cavities. Bone regeneration and graft resorption were significantly greater in defects grafted with BG-HCA than in defects grafted with BG-ACP or UBG. The rapid bone regeneration associated with pretreated BG could be explained by the ability of the HCA layer to enhance the selective adsorption of attachment proteins and growth factors which stimulate osteoblast adhesion and bone deposition.⁸ The activity of these adsorbed proteins persisted longer on the surface-modified bioactive glass than on the UBG surface.^{15,16} Another mechanism by which the surface-modified bioactive glass could enhance bone formation is through ion release from

its surface, as supported by the work of Matsuoka and associates.⁹

In addition to its favorable effects on the ability of bioactive glass to regenerate bone, surface modification also enhanced graft material resorption. There was significantly more resorption with BG-ACP than with UBG; there was significantly more resorption with BG-HCA than with BG-ACP. The resorption of bioactive glass in vivo is primarily controlled by the material's stability in tissue fluid and the cellular activity. The duration of immersion treatment before bioactive glass implantation controls the thickness and the structure of the layer that forms on the surface of bioactive glass. Longer immersion duration resulted in the transformation

of the thin ACP layer into a relatively thick HCA layer. The apatite layer was poorly crystallized, defective, and calcium deficient.

Results of the present study suggested that these properties of the HCA facilitate material degradation and phagocytosis by cells. The kind of cells involved in the resorption process still needs to be elucidated. However, a significantly greater rate of bone regeneration was associated with BG-HCA resorption, which indicates that the resorption process is primarily cell mediated, although solution-mediated resorption cannot be excluded. On the other hand, dissolution-precipitation reactions at the interface of UBG and tissue fluids are hindered by protein adsorption.⁸ Protein adsorption also interferes with the mechanism of bioactivity that leads to the formation of the HCA layer. Consequently, the resorption of the relatively rigid silica network of UBG by either mechanism will be sluggish compared to the resorption of BG-HCA.

Digital radiographic imaging showed significant differences in the density of the bony defects in the initial phase of healing. While the density of grafted defects significantly increased, that of the ungrafted defects markedly decreased. Many events occurring in the bony defect can have a significant impact on density measurement. For example, deposition of new bone tissue has the potential to increase radiographic density. Many studies have demonstrated an increase in radiographic density 4 to 6 months postsurgery because of bone filling in ungrafted defects.^{17,18} The level of radiopacity increased even further throughout the 6-month observation period. On the other hand, the resorption of the graft material and/or the host bone has the potential to decrease the measured density. Therefore, the change in density inside the grafted defects is the summation of the 2 processes, material resorption and new bone tissue deposition.

In the present study, the initial increase in the density of grafted cystic bone defects likely indicates that bone tissue regeneration is the dominating process. Between 2 and 4 weeks postsurgery, the rate of increase in density in the defects grafted with BG-HCA was more than twice that in defects grafted with UBG. This may indicate that the creation of the HCA layer on the surface of bioactive glass before implantation significantly enhanced bone tissue regeneration clinically. Measurements of density of the grafted cystic cavities suggested that bone deposition continued to dominate inside the defect up to 16 weeks postsurgery. At this point, bone had almost completely filled the spaces between the graft particles. After 16 weeks, the density of the cystic cavity started to decrease, indicat-

ing that graft material resorption may have started to dominate. This suggestion correlates with the histologic results, which showed that defects grafted with BG-HCA were backed with well-developed bone trabeculae incorporating remnants of the graft material.

However, the radiographic density of defects filled with UBG continued to increase until week 24, indicating continuation of bone tissue deposition inside the cavity. The incomplete bone filling inside defects grafted with unmodified bioactive glass 6 months postsurgery is in agreement with many studies in the literature. Low and colleagues and Zamet and colleagues described studies in which the bone formation process in cavities filled with UBG particles was incomplete 1 year postsurgery.^{19,20} Incomplete bone formation inside the defect correlates well with the histologic results, which showed that the interspaces between UBG particles were filled mainly with bone cells (Fig 1). The limited bone conductivity of UBG compared to BG-HCA at this point in time could be attributed to the non-uniform formation of the CaP surface layer on UBG.

Density measurements of ungrafted control cystic defects showed a decrease up to 8 weeks, after which the density values increased continuously until week 24. The initial decrease in density probably indicated that bone resorption was the dominating process until week 8. This observation was expected, as bone resorption usually precedes bone tissue formation in the normal bone healing process. Other studies in the literature have indicated that a slight change in the radiographic appearance of ungrafted defects may be observed 8 weeks postoperative.²¹ After 8 weeks, the density continued to increase until week 24, indicating new bone tissue formation. This healing phase is similar to the so-called "trabecular pattern" which occurs after 6 months with partial filling of the defect with bone.²¹

CONCLUSION

Surface modification of bioactive glass before implantation significantly enhanced bone tissue regeneration and graft material resorption. Bioactive glass covered with an HCA layer enhanced bone tissue regeneration better than bioactive glass covered with ACP or control UBG. In conjunction with the enhanced bone tissue formation, a significant decrease in the amount of surface-modified bioactive glass present in the bony defect was seen. This observation indicates that creation of a calcium phosphate layer on the bioactive glass surface might

enhance cell-mediated resorption of the material. This clinical study showed the superiority of surface-modified bioactive glass over the traditional unmodified material in accelerating bone tissue regeneration in cystic bone defects. The change in density measurements inside the cystic bone defects correlates well with bone regeneration and graft material resorption observed *in vivo*. Results of both clinical and animal studies suggested that the use of surface-modified bioactive glass covered with an HCA layer has the potential to accelerate bone formation and graft material resorption better than UBG.

REFERENCES

1. Damien CJ, Parsons JR. Bone graft and bone graft substitutes: A review of current technology and applications. *J Appl Biomater* 1991;2:187-208.
2. Habal MB, Reddi AH. Different forms of bone grafts. In: Habal MB, Reddi AH (eds). *Bone Grafts and Bone Substitutes*. Philadelphia: Saunders, 1992:6-8.
3. Hench LL, Wilson J (eds). *An Introduction to Bioceramics*. Singapore: World Scientific, 1993.
4. Hench LL. Bioceramics: From concept to clinic. *J Am Ceram Soc* 1991;74:1487-1510.
5. Andersson OH, Kangasniemi I. Calcium phosphate formation at the surface of bioactive glass *in vitro*. *J Biomed Mater Res* 1991;25:1019-1030.
6. Kim CY, Clark AE, Hench LL. Early stages of calcium phosphate layer formation in bioglasses. *J Noncryst Solids* 1989;113:195-202.
7. El-Ghannam A, Ducheyne P, Shapiro IM. Bioactive material template for *in vitro* synthesis of bone. *J Biomed Mater Res* 1995;29:359-370.
8. El-Ghannam A, Ducheyne P, Shapiro I. Effect of serum proteins on osteoblast adhesion to surface-modified bioactive glass and hydroxyapatite. *J Orthop Res* 1999;17:340-345.
9. Matsuoka H, Akiyama H, Okada Y, et al. *In vitro* analysis of the stimulation of bone formation by highly bioactive apatite- and wollastonite-containing glass-ceramic: Released calcium ions promote osteogenic differentiation in osteoblastic ROS17/2.8 cells. *J Biomed Mater Res* 1999;47:176-188.
10. Kokubo T, Ito S, Huang ZT, et al. CaP-rich layer formed on high-strength bioactive glass-ceramic A-W. *J Biomed Mater Res* 1990;24:331-343.
11. Miyaji F, Kim H, Handa S, Kokubo T, Nakamura T. Bone-like apatite coating on organic polymers: Novel nucleation process using sodium silicate solution. *Biomaterials* 1999;20:913-919.
12. Layrolle P, van Blitterswijk CA, De Groot K. Biomimetic hydroxyapatite coating on Ti-6Al-4V induced by pre-calcification. In: LeGeros RZ, LeGeros JP (eds). *Bioceramics. Vol 11: Proceedings of the 11th International Symposium on Ceramics in Medicine*, New York, November 1998. Cologne: German Ceramic Society, 1999:465-468.
13. de Bruijn JD, van Blitterswijk CA. New developments in implant coatings: Biomimetic and tissue engineering. *Biomater Surg* 1998;77-82.
14. Russ JC (ed). *The Image Processing Handbook*, ed 3. Boca Raton: CRC Press, 1992:288,395.
15. Lobel KD, Hench LL. *In vitro* protein interactions with a bioactive gel-glass. *J Sol-Gel Sci Tech* 1996;7:69-76.
16. Lobel KD, Hench LL. *In vitro* adsorption and activity of enzymes on reaction layers of bioactive glass substrates. *J Biomed Mater Res* 1998;39:575-579.
17. Yoshioko T, Kobayashi G, Suda H, Sasaki T. Quantitative subtraction with direct digital dental radiography. *Dento-maxillofac Radiol* 1992;26:286-294.
18. Wheeler DL, Stokes KF, Park HM, Hollinger JO. Evaluation of particulate Bioglass in rabbit radius osteotomy model. *J Biomed Mater Res* 1997;35:249-251.
19. Low SB, King CJ, Krieger J. An evaluation of bioactive ceramic in the treatment of periodontal osseous defects. *Int J Periodontics Restorative Dent* 1997;17:359-367.
20. Zamet JS, Darbar UR, Griffiths GS, et al. Particulate bioglass as a grafting material in the treatment of periodontal intrabony defects. *J Clin Periodontol* 1997;24:410-418.
21. Kawai T, Murakami S, Hiranuma H, Sakuda M. Healing after removal of benign cysts and tumors of the jaw. A radiological appraisal. *Oral Surg Oral Med Oral Pathol Oral Radiol Endod* 1995;79:517-525.